ADVANCED MATERIALS

Table 2. Summary of the nonlinear optical properties for compounds **1–5** in toluene.

Sample	*Conc.* [g L^{-1}]	α_0 [cm^{-1}]	κ σ_{ex}/σ_0	F_{sat} [J cm^{-2}]
1	0.5	1.10	13.5 ± 0.4	27.0 ± 1.0
2	0.5	0.91	13.6 ± 0.4	8.4 ± 1.0
3	0.5	0.53	27.4 ± 0.6	24.2 ± 0.8
4	0.5	0.93	14.8 ± 0.3	7.0 ± 0.2
5	0.5	0.93	12.5 ± 0.4	9.8 ± 0.5

[tBu$_4$PcIn]$_2$O are almost identical despite the difference in their saturation energy densities.

In summary, spectroscopic data and excited relaxation data of the In- and Ga-Pcs employed in the present study do not show aggregation phenomena to reduce the effective nonlinear absorption.[8,13] The optical limiting in these compounds is very effective compared to other phthalocyanines[18] exhibiting a range of saturation densities and absorption cross-section ratios. Axial substitution of the *p*-TMP functional group at the central gallium and indium in **1** and **3** results in a reduction of the saturation energy density by a factor in excess of **3**. This method of tailoring the saturation of the optical limiters will prove to be very useful in the construction of passive organic optical limiters where multiple layers of effective absorbers with decreasing saturation may be desirable.

Experimental

The synthesis and structural characterization of compounds **1–5** have been previously reported [9,11,12]. All solvents used were purified, dried and distilled under dry nitrogen. UV-vis spectra were recorded in Shimadzu UV-365. Fluorescence spectra and lifetimes were measured by a single-photon counting method using an argon ion laser, a pumped Ti:sapphire laser (Spectra-Physics, Tsunami 3960, FWHM 150 fs) with a pulse selector (Spectra-Physics, 3980), a second harmonic generator (Spectra-Physics, GWU-23PS), and a streakscope (Hamamatsu Photonics, C4334-01). Each sample was excited in toluene with 410 nm laser light.

The open aperture of a *Z*-scan experiment [16] was used to measure the optical limiting response in the samples. All experiments described in this study were performed using 6 ns 532 nm laser light pulses from a Q switched frequency doubled Nd:YAG laser with a pulse repetition rate of 10 Hz. The beam was spatially filtered to remove the higher order modes and tightly focused using a 9 cm focal length lens. All samples were measured in quartz cells with a 1 mm optical path length, and at concentrations of 0.5 g L^{-1} (~ 10^{-4} M) in toluene.

Received: October 2, 2002
Final version: February 10, 2003

[1] H S. Nalwa, J. S. Shirk, in *Phthalocyanines: Properties and Applications* (Eds: C. C. Leznoff, A. B. P. Lever), Vol. 4, John Wiley and Sons, New York **1996**, pp. 79–181.
[2] G. de la Torre, P. Vázquez, F. Agulló-López, T. Torres, *J. Mater. Chem.* **1998**, *8*, 1671.
[3] a) M. Hanack, T. Schneider, M. Barthel, J. S. Shirk, S. R. Flom, R. G. S. Pong, *Coordination Chem. Rev.* **2001**, *219–221*, 235. b) D. Dini, M. Barthel, M. Hanack, *Eur. J. Org. Chem.* **2001**, *20*, 3759.
[4] C. G. Claessens, W. J. Blau, M. Cook, M. Hanack, R. J. M. Nolte, T. Torres, D. Wöhrle, *Monatsh. Chem.* **2001**, *132*, 3.
[5] J. W. Perry, K. Mansour, I. Y. S. Lee, X. L. Wu, P. V. Bedworth, C. T. Chen, D. Ng, S. R. Marder, P. Miles, T. Wada, M. Tian, H. Sasabe, *Science* **1996**, *273*, 1533.
[6] D. R. Coulter, V. M. Miskowski, J. W. Perry, T. H. Wei, E. W. Van Stryland, D. J. Hagan, *SPIE Proc.* **1989**, *1105*, 42.
[7] J. S. Shirk, R. G. S. Pong, F. J. Bartoli, A. W. Snow, *Appl. Phys. Lett.* **1993**, *63*, 1880.
[8] J. S. Shirk, R. G. S. Pong, S. R. Flom, H. Heckmann, M. Hanack, *J. Phys. Chem. A* **2000**, *104*, 1438.
[9] M. Hanack, H. Heckmann, *Eur. J. Inorg. Chem.* **1998**, 367.
[10] T. Schneider, H. Heckmann, M. Barthel, M. Hanack, *Eur. J. Org. Chem.* **2001**, 3055.
[11] Y. Chen, L. R. Subramanian, M. Barthel, M. Hanack, *Eur. J. Inorg. Chem.* **2002**, 1032.
[12] Y. Chen, M. Barthel, M. Seiler, L. R. Subramanian, H. Bertagnolli, M. Hanack, *Angew. Chem.* **2002**, *114*, 3373; *Angew. Chem. Int. Ed.* **2002**, *41*, 3239.
[13] A. W. Snow, J. S. Shirk, L. H. Peebles Jr., in *Proc. of the Int. Conf. on Porphyrins and Phthalocyanines-Symposium Lectures*, Dijon, France, June **2000**, pp. 177.
[14] a) Y. Sakakibara, R. N. Bera, T. Mizutani, K. Ishida, M. Tokumoto, T. Tani, *J. Phys. Chem. B* **2001**, *105*, 1547. b) J. H. Brannon, D. Magde, *J. Am. Chem. Soc.* **1980**, *102*, 62. c) F. L. Plows, A. C. Jones, *J. Mol. Spectrosc.* **1999**, *194*, 163.
[15] a) M.Fujitsuka, O. Ito, H. Konami, *Bull. Chem. Soc. Jpn.* **2001**, *74*, 1. b) Y. Chen, Z. E. Huang, R. F. Cai, B. C. Yu, O. Ito, J. Zhang, W. W. Ma, C. F. Zhong, L. Zhao, Y. F. Li, L. Zhu, M. Fujitsuka, A. Watanabe, *J. Polym. Sci. B: Polym. Phys.* **1997**, *35*, 1185.
[16] M. Sheik-Bahae, A. A. Said, T.-H. Wei, D. J. Hagan, E. W. Van Stryland, *IEEE J. Quantum Electron.* **1990**, *26*, 760.
[17] F. Z. Henari, W. J. Blau, L. R. Milgrom, G. Yahioglu, D. Phillips, J. A. Lacey, *Chem. Phys. Lett.* **1997**, *267*, 229.
[18] S. M. O'Flaherty, S. V. Hold, M. J. Cook, T. Torres, Y. Chen, M. Hanack, W. J. Blau, *Adv. Mater.* **2003**, *15*, 19.
[19] Y. Chen, L. R. Subramanian, M. Fujitsuka, O. Ito, S. M. O'Flaherty, W. J. Blau, T. Schneider, D. Dini, M. Hanack, *Chem. Eur. J.* **2002**, *8*, 4248.

Assemblies of Metal Nanoparticles and Self-Assembled Peptide Fibrils—Formation of Double Helical and Single-Chain Arrays of Metal Nanoparticles**

By *Xiaoyi Fu*, *Yuan Wang*,* *Lixin Huang*, *Yinlin Sha*,* *Linlin Gui*, *Luhua Lai*, and *Youqi Tang*

There is growing interest in attempts to combine biomaterials and inorganic nanoparticles and investigating their properties. One of the research motivations for this combination is to take advantage of the well-defined structures and special properties of biomolecules and their supermolecular structures to organize the nanoparticles into predefined, topologically intricate nanostructures or to synthesize miscellaneous materials for potential applications in electronic, optical, and chemical devices.[1] Several kinds of biomaterials have been

[*] Prof. Y. Wang, Dr. X. Fu, Prof. L. Gui, Prof. L. Lai, Prof. Y. Tang
State Key Laboratory for Structural Chemistry of Unstable and Stable Species, College of Chemistry & Molecular Engineering
Peking University
Beijing 100871 (P.R. China)
E-mail: wangy@pku.edu.cn
Dr. Y. Sha, L. Huang
Single Molecule & Nano-Biomedicine Laboratory, Department of Biophysics, School of Basic Medical Sciences, Peking University
Beijing 100083 (P.R. China)
E-mail: shyl@bjmu.edu.cn

[**] This work was financially supported by the Major State Basic Research Development Program (project No. G2000077503) from the Chinese Ministry of Science and Technology and by grants from NSFC (projects No. 29925308, 90206011, 20273002, 20103001).

  DOI: 10.1002/adma.200304624

used as templates for this purpose, for example, tobacco mosaic virus and bacterial S-layers have been used for the generation of ordered arrays of metal and semiconductor nanoparticles,[2,3] and DNA molecules have been used to mediate assembly of metal nanoparticles into linear, monolayer, and multilayer structures.[4–7] In addition, DNA molecules have also been used to prepare metal nanowires.[8,9] On the other hand, studies on the special conformational transition behavior or misfolding of proteins are of great importance because the deposition of insoluble amyloid plaque or fibril is a hallmark of a group of neurodegenerative diseases, such as Alzheimer's disease (AD) and Parkinson's disease,[10–14] which are usually termed protein conformational diseases.[15,16] It has been known that some short peptides can also self-assemble into fibrous structures under appropriate conditions.[17] This provides not only a possible way to simulate the fibrosis process of proteins but also a new type of biomolecular templates for assembling small nanoparticles. To our knowledge, studies on the assembly of metal nanoparticles on peptide fibrils have been scarce until now.

In this paper, we report the metallization of a new kind of peptide nanofibril that was derived from the self-assembly of a synthesized peptide of 12 residues (T1) (see structure below). Deposition of Au and Pd nanoparticles on the T1 peptide fibrils, which have an average diameter of about 10 nm and length of several micrometers, was conducted. We have succeeded in preparing double helical arrays and single-chain arrays of metal nanoparticles using the peptide fibrils as templates for the first time. Continuous Pd nanowires derived from stacking the metal nanoparticles along the fibrils were also successfully prepared. It was found that the pH of the reaction media and size of the metal nanoparticles have an obvious influence on the structure of the assemblies.

Assemblies of Au Nanoparticles and T1 Fibril: Transmission electron microscopy (TEM) of the T1 fibril stained with uranyl acetate (Fig. 1a), which was prepared according to the method described in the Experimental section, shows that the fibrils have a fibrous structure with length up to several micrometers and an average diameter of about 10 nm. However, the detailed structure of the T1 fibril cannot be seen due to its low contrast in the TEM image. Au colloidal particles prepared in this work have an average diameter of 3.6 nm with a size distribution ranging from 2 to 6 nm as shown in Figure 1b.

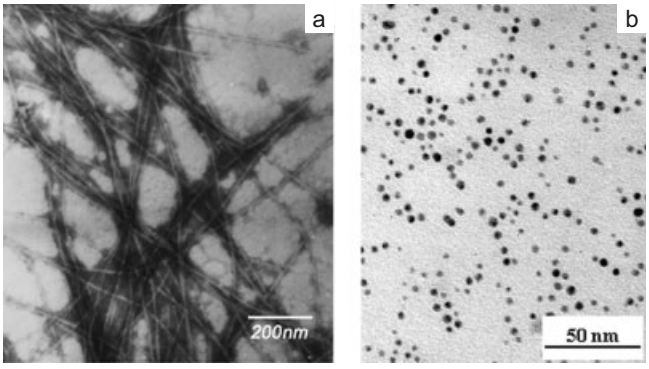

Fig. 1. TEM images of the prepared T1 fibrils (a) and Au colloidal particles (b).

It is well known that metal colloidal nanoparticles are usually negatively charged because of the adsorption of anionic stabilizer. Therefore, if the surfaces of T1 fibrils were positively charged due to the protonation of N-containing groups in the T1 molecules, the metal nanoparticles would self-assemble at the surfaces of the T1 fibrils through electrostatic interactions.

Figure 2 shows a TEM image of a T1-fibril/Au-nanoparticle assembly (T1–Au fibril) prepared by mixing a colloidal solution of T1 fibril and a Au colloidal solution at pH 6. It can be seen from Figure 2 that Au nanoparticles anchored on the T1 fibril template are 2–6 nm in diameter, and are quite similar to those in the Au colloidal solution (see Fig. 1b). The lengths of these T1–Au fibrils range from several hundreds of nano-

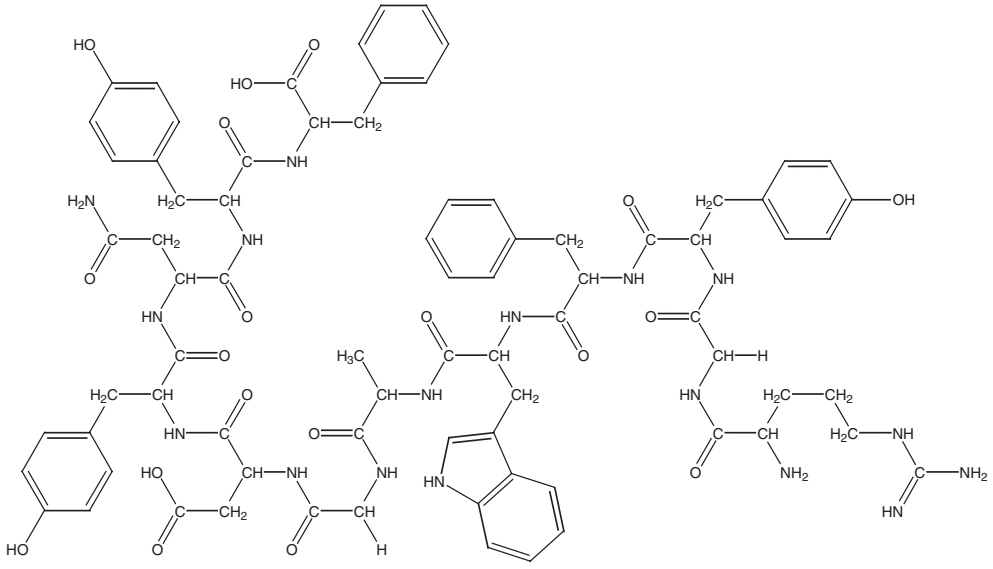

ADVANCED MATERIALS

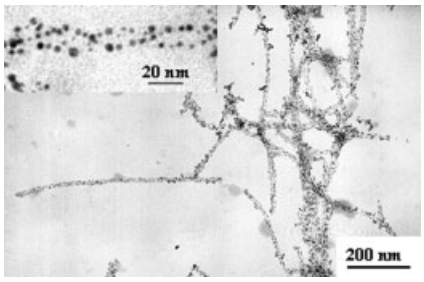

Fig. 2. TEM images of Au–T1 assemblies obtained at pH 6. Inset is a high-magnification image of a double helical array of Au nanoparticles.

meters to several micrometers. The high-magnification image of an individual T1–Au fibril shown in the inset of Figure 1 reveals that Au nanoparticles on T1 fibril do not disperse randomly on the surface of the template but align along the template forming double helical patterns. The distance between the opposite Au nanoparticles, perpendicular to the T1–Au fibril, is about 10 nm, which is consistent with the diameter of T1 fibril shown in Figure 1. The two strings of Au nanoparticles twist along the fibril axis with a periodicity of about 30 to 40 nm.

Au nanoparticles with different particle sizes were used to label T1 fibril in order to study the influence of metal particle size on the assembly structure. It was found that small particles benefited the formation of clear and integrated double helical arrays of Au nanoparticles. When large Au particles, especially those having an average diameter larger than 10 nm, were used, random distribution of metal nanoparticles on T1 fibril appeared more frequently. The reason is obvious: Because the diameter of the T1 fibril template is 10 nm, it is hard for large nanoparticles to deposit on both sides of T1 fibril simultaneously owing to electrostatic repulsion between the colloidal metal nanoparticles.

It was found that the pH value of the reaction media could influence the structure of the Au–T1 assembly dramatically. The colloidal solution of T1 fibril was mixed with the Au colloidal solution and the mixture was kept under different pH conditions for a period of time until the Au–T1 assemblies precipitated. The color of the mixed colloidal solution became darker and precipitate appeared readily under acidic conditions, whereas under alkali conditions, precipitate hardly appeared.

Figures 3a,b show TEM images of Au–T1 assemblies prepared at a pH of 3.5 and 4.5, respectively. An interesting observation was that only single-chain arrays instead of double helical arrays of Au nanoparticles were obtained at a pH value of 3.5 (Fig. 3a). However, as shown in Figure 2, only double helical arrays of Au nanoparticles were observed at a pH value of 6. When pH was adjusted to 4.5, both single-chain arrays and double helical arrays of Au nanoparticles could be observed, although the single-chain arrays appeared more frequently (Fig. 3b).

In the single-chain arrays shown in Figure 3a, the average spacing between the Au nanoparticles is less than 0.7 nm, which is smaller than that in the double helical arrays (about

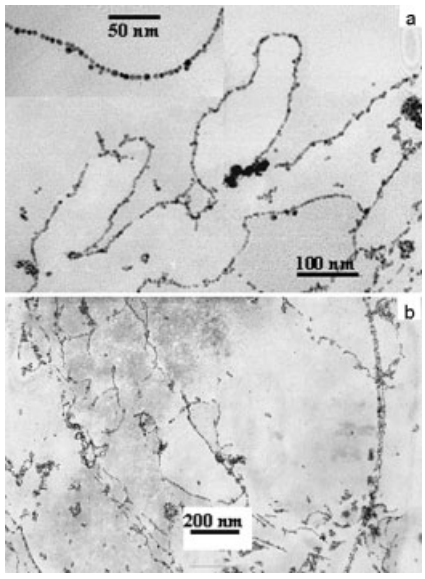

Fig. 3. TEM images of Au–T1 assemblies obtained at different pH values. a) ≈ pH 3.5; the inset is a high-magnification image of a single-chain array of well-separated Au nanoparticles. b) ≈ pH 4.5.

1.3 nm, along the particle strings as shown in Fig. 2). In addition, it was also observed that the diameter and the length of periodicity of the helical arrays were affected by pH. For example, in the T1–Au fibril obtained at pH 4.5, the distance between the opposite Au particles perpendicular to the axis is 12–17 nm, and the length of periodicity is 40–50 nm, which are larger than the corresponding values of the helical arrays obtained at pH 6.

Marini et al.[17] have observed a helical ribbon structure in a self-assembled peptide fibril derived from KFE8 (FKFEFKFE) peptide using atomic force microscopy. A molecular dynamics simulation study suggests that the KFE8 fibril has a left-handed double helical β-sheet structure. Au colloidal particles have been used as a dye for the TEM investigation of the inner structure of cells for 10 to 15 years owing to their biocompatibility and high contrast in the TEM.[18] From the assembled patterns of Au nanoparticles on T1 fibril, we can speculate that the T1 fibril has a helical structure at ~ pH 6, which disappears at ~ pH 3.5. Details of the structure and pH dependence of the T1 fibril are the subject of further investigation. One possibility is that the peptide fibril at pH 6 consists of two fibers wrapped around each other, which dissociate into two separate fibers at ~ pH 3.5. This is a reasonable model that accounts for the observed results.

Assemblies of Pd Nanoparticles and Formation of Pd Nanowires: Pd nanoparticles were assembled onto T1 fibril by reducing Pd^{II} ions with hydrogen in the presence of T1 fibrils. The chemical deposition of palladium onto the T1 fibril also led to the formation of double-helical arrays and single-chain arrays of Pd nanoparticles, as shown in Figure 4. Figure 4a shows that well-separated Pd nanoparticles, nearly spherical in shape and 3–8 nm in diameter, are aligned along the T1 fibril template forming an obvious double helical structure, in which the distance between the opposite Pd particles perpen-

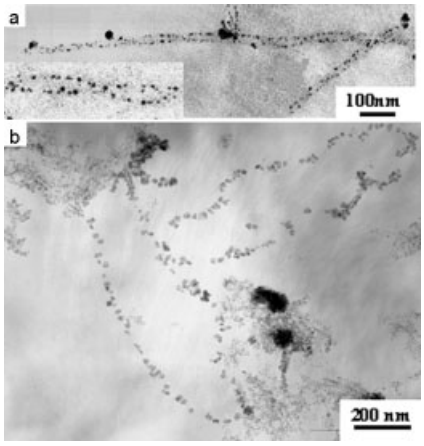

Fig. 4. TEM images of assemblies of Pd nanoparticles and T1 fibrils. a) Double helical arrays of Pd nanoparticles; inset is a high-magnification image. b) Single-chain arrays of Pd nanoparticles.

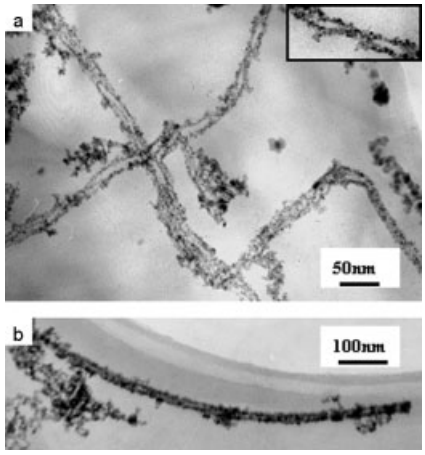

Fig. 5. TEM images of Pd nanowires of different shapes based on T1 fibrils. The inset shows the helical structure at higher magnification.

dicular to the axis is about 22 nm, while the length of helical periodicity varies from 90 to 120 nm. Figure 4b shows the TEM image of single-chain arrays of Pd nanoparticles, in which the Pd nanoparticles have irregular shapes and their diameters range from 8 to 26 nm.

In the Pd metallization process adopted in this work, there may exist two kinds of Pd nucleation mechanisms. One is the reduction of Pd^{II} ions coordinated to the ligands on the surface of T1 fibril and formation of small Pd clusters by aggregation of the produced Pd atoms. The initially formed Pd clusters then catalyze the reduction of Pd ions at their surfaces, resulting in further deposition of Pd atoms. The second mechanism is via a nucleation process occurring in solution, i.e., reducing Pd ions dissolved in solution with hydrogen and forming Pd nanoparticles that could be attached to the surface of T1 fibril by charging or coordination interactions. From our experience, we believe that Pd metal nanoparticles derived from the second mechanism should be larger in size and wider in distribution than those formed through the first mechanism.

Comparing the double helical arrays of Pd nanoparticles with those of Au nanoparticles, it can be seen that the former have better structural integrity. In addition, both the helical diameter and the length of periodicity of Pd nanoparticle arrays are larger than those of the Au nanoparticle arrays. The reduction of Pd^{II} ions is accompanied by a decrease in pH ($Pd^{II} + H_2 \longrightarrow Pd^0 + 2H^+$), which may partly be responsible for the larger values of the diameter and length of helical periodicities observed in the double helical arrays of Pd nanoparticles.

When a $PdCl_2$ solution was repeatedly added to a suspension of T1–Pd fibril followed by reduction of Pd^{II} ions with hydrogen each time, Pd nanoparticles grew and more Pd particles aggregated on the template, resulting in the formation of continuous Pd nanowires. Depending on the amount of deposited Pd, different Pd nanowires could be obtained. In this process, the initially formed Pd nanoparticles served as a catalyst for the further reduction of Pd ions. Figure 5 shows TEM images of Pd nanowires of different shapes. When the amount of Pd loading was not very large, the helical structure formed by the two inter-twisted strips of Pd nanoparticles could still be seen clearly (Fig. 5a). Further increase in the amount of Pd deposited led to occupation of the vacancies in the preformed nanowires by Pd nanoparticles, resulting in continuous Pd nanowires as shown in Figure 5b.

In summary, this paper describes the assembly of Au and Pd nanoparticles on a new peptide fibril template derived from self-assembled molecules. Double helical arrays of Au and Pd nanoparticles were obtained for the first time at ~pH 6, whereas, only single-chain arrays of Au nanoparticles formed at ~pH 3.5. The diameter and length of the double helical arrays of metal nanoparticles are affected by the acidity of the reaction medium. Small metal nanoparticles benefit the formation of a clear and integrated double helical structure. The patterns of metal nanoparticle arrays suggest that at pH 6, the T1 nanofibril has a helical structure that disappears under acidic conditions of ~pH 3.5. Pd nanowires of different shapes were prepared by varying the amount of metal deposition. This work provides a new way to construct valuable nanostructures. The double helical and single-chain arrays of separated small Au nanoparticles as well as the Pd nanowires are interesting building blocks for the preparation of new functional nanostructured devices.

Experimental

Materials and Instrumentation: 9-Fluorenylmethoxycarbonyl amino acids, including FmocAla, FmocGly, FmocPhe, FmocTrp, FmocAsn, FmocAsp (^{t}Bu), FmocTyr (^{t}Bu), FmocArg (Mtr), and FmocThr (^{t}Bu) are products of ACT (USA). Chloroauric acid ($HAuCl_4$, AR grade), palladium chloride ($PdCl_2$, AR grade), and H_3citrate were purchased from Beijing Chemical Reagents Company. Na_3citrate, NaOH, and $NaBH_4$ were obtained from Beijing Chemical Products. Organic solvents and the other chemicals of AR grade were used as received. Ultrapure water (18 MΩ) was used in this work.

Transmission Electron Microscopy: TEM images were taken on a JEM 2000 FX electron microscope operated at 120 kV. Samples were prepared by dropping a corresponding suspension of the metallized T1 fibril onto a copper grid coated with a polymer film.

ADVANCED MATERIALS

Preparation of the Self-Assembled T1 Nanofibril: T1 was synthesized by a solid-phase synthetic method based on Fmoc chemistry. The first amino acid Phe was loaded to Wang resin (substitution, 0.8 mmol g^{-1}) by the preformed symmetrical anhydride method using *N,N*-dimethylaminopyridine as a catalyst. 2-(1H-Benzotriazol-1-yl)-1,1,3,3-tetramethyl uranium hexafluorophosphate/1-hydroxy-benzotrizole (HBTU/HOBT) was employed as the coupling reagent. The peptide product was cleaved from the resin using K reagent (82.5 % TFA, 5 % thioanisole, 2.5 % ethanedithiol,<Seitenzahl> 5 % phenol, and 5 % H_2O), purified by RP-HPLC (Gilson Inc., France, zorbax C_{18} column, 9.4 × 250 mm), and confirmed by MALDI-TOF mass spectrometry ([M+H]: observed 1562.0/ calc. 1558.7).

Incubation of T1 in phosphate buffered saline (PBS) at 37 °C for 2 weeks resulted in T1 fibril as confirmed by TEM. The TEM sample was prepared by transferring a colloidal solution of T1 fibril onto a TEM grid coated with a carbon film. After drying, the sample was stained with uranyl acetate.

Preparation of Au Colloids: A Au colloidal solution was prepared according to the procedure described by Brown et al. [19]. 0.5 mL of a $HAuCl_4$ solution (2 %) and 2 mL of a Na_3citrate solution (38.8 mM) were added to 90 mL of H_2O. After about 1 min stirring, 1 mL of freshly prepared $NaBH_4$/Na_3citrate aqueous solution (13 mg $NaBH_4$ in 5 mL of a Na_3citrate solution (38.8 mM)) was added. A transparent ruby-red colloidal solution formed immediately, which was stirred for a further 30 min and stored at 4 °C. The pH value of the prepared Au colloidal solution was about 6. The UV-vis absorption spectrum of the Au sol exhibited a surface plasmon band at 522 nm.

Assembly of Au Nanoparticles on T1 Fibril: The preformed Au nanoparticles were attached to the T1 fibril template by a simple procedure. A typical experiment involved adding 5 μL of T1 fibril colloidal solution into 0.5 mL of the Au colloidal solution. After keeping the mixture at 4 °C for 24 h, a red precipitate appeared, indicating that Au nanoparticles had been attached onto the T1 fibrils. The precipitate was isolated by centrifuging at 4000 rpm for 30 min and then dispersed in H_2O by ultrasonic treatment for several seconds. The obtained suspension was used in the preparation of TEM samples. To investigate the effect of pH on the structure of the Au nanoparticle assembly, the pH value of the obtained mixed colloidal solution was adjusted to pH 3.5, 4.5, 5.4, 6.5, and 9 by adding different amounts of a H_3citrate solution (0.1 M) or a NaOH solution (0.1 M).

Assembly of Pd Nanoparticles onto T1 Fibril: To assemble Pd nanoparticles, a different strategy was adopted. A saturated aqueous solution of $PdCl_2$ was prepared by adding excessive amount of $PdCl_2$ in ultra-pure water and then treating the mixture in an ultrasonic bath for 10 min. The mixture was centrifuged for 10 min at 4000 rpm to separate undissolved $PdCl_2$. The obtained $PdCl_2$ solution was mixed with the colloidal solution of T1 fibril in a ratio of 1:1 and then a five-fold excess of Na_3citrate aqueous solution (0.001 M) was added to the mixture. After standing for several hours, the above mixture was exposed to hydrogen atmosphere for several hours. The color of the solution became yellow at the beginning, and then brown precipitate appeared, indicating that Pd^{II} had been reduced by hydrogen and the formed Pd nanoparticles were bound onto the T1 fibril template. Similarly, the produced precipitate was isolated by centrifuging and then re-suspended in H_2O to prepare the TEM samples. In order to obtain a continuous nanowire of Pd nanoparticles, the process of adding the $PdCl_2$ solution into the suspension of Pd-nanoparticle/T1-fibril complex and then reduction of Pd^{II} with hydrogen was repeated several times.

Received: November 15, 2002
Final version: February 25, 2003

[1] C. M. Niemeyer, *Angew. Chem. Int. Ed*. **2001**, *40*, 4128.
[2] M. Mertig, R. Kirsch, W. Pompe, H. Engelhardt, *Eur. Phys. J. D* **1999**, *9*, 45.
[3] a) U. B. Slytr, P. Messner, D. Pum, M. Sara, *Angew. Chem. Int. Ed*. **1999**, *38*, 1034. b) W. Shenton, D. Pum, U. B. Sleytr, S. Mann, *Nature* **1997**, *389*, 585. c) W. Shenton, T. Douglas, M. Young, G. Stubbs, S. Mann, *Adv. Mater.* **1999**, *11*, 253.
[4] M. Sastry, A. Kumar, S. Datar, C. V. Dharmadhikari, K. N. Ganesh, *Appl. Phys. Lett*. **2001**, *78*, 2943.
[5] Y. Maeda, H. Tabata, T. Kawai, *Appl. Phys. Lett*. **2001**, *79*, 1181.
[6] T. A. Taton, R. C. Mucic, C. A. Mirkin, R. L. Letsinger, *J. Am. Chem. Soc.* **2000**, *122*, 6305.
[7] E. Dujardin, L.-B. Hsin, C. R. C. Wang, S. Mann, *Chem. Commun.* **2001**, 1264.
[8] E. Braun, Y. Eichen, U. Sivan, G. Ben-Yoseph, *Nature* **1998**, *391*, 775.
[9] a) J. Richter, R. Seidel, R. Kirsch, M. Mertig, W. Pompe, J. Plaschke, H. K. Schackert, *Adv. Mater.* **2000**, *12*, 507. b) J. Richter, M. Mertig, W. Pompe, I. Monch, H. K. Schackert, *Appl. Phys. Lett*. **2001**, *78*, 536.
[10] J. Hardy, G. Katrina, *Science* **1998**, *282*, 1075.
[11] R. S. Hegde, J. A. Mastrianni, M. R. Scott, K. A. DeFea, P. Tremblay, M. Torchia, S. J. DeArmond, S. B. Prusiner, V. R. Lingappa, *Science* **1998**, *279*, 827.
[12] D. J. Selkoe, *Science* **1997**, *275*, 630.
[13] C. Haass, P. J. Kahle, *Nature* **2000**, *404*, 341.
[14] S. B. Prusiner, *Science* **1997**, *278*, 245.
[15] R. W. Carrell, D. A. Lomas, *Lancet* **1997**, *350*, 134.
[16] R. W.Carrell, B. Gooptu, *Curr. Opin. Struct. Biol.***1998**, *8*, 799.
[17] D. M. Marini, W. Hwang, D. A. Laufferburger, A. Zhang, R. D. Kammar, *Nano Lett*. **2002**, *2*, 295.
[18] J. De Mey, in *Immunocytochemistry: Modern Methods and Application* (Eds: J. Polak, S. Van Nooden), Wright-PSG, Bristol **1986**.
[19] K. R. Brown, D. G. Walter, M. J. Natan, *Chem. Mater.* **2000**, *12*, 306.

Stimulated Emission from a Needle-like Single Crystal of an End-Capped Fluorene/Phenylene Co-oligomer**

By *Xuhui Zhu*, *Denis Gindre*, *Nicolas Mercier*,* *Pierre Frère*, and *Jean-Michel Nunzi**

Recent advances in optically pumped solid organic lasers have been achieved with a variety of semiconducting conjugated polymers[1–3] and dye-doped molecular solids as gain media[4,5] in thin (neat) films, triggered by the observation of lasing in a liquid solution of poly(2-methoxy-5-(2′-ethylhexyloxy)-1,4-phenylene vinylene).[6] The fabrication of an organic diode laser is still a research target and only materials with large mobilities for both electrons and holes are serious candidates. On account of their high purity and their rigorously defined structure, high-quality molecular single crystals are more advantageous than polymers in this respect. Additionally, single crystals do not display grain boundary defects associated with solution-processed thin films (e.g., prepared by spin-coating) which may serve as carrier traps. Optically induced lasing from pure anthracene single crystals was reported as early as 1974.[7] Amplified spontaneous emission (ASE), which can be called a mirrorless laser emission, from one photopumped oligomeric single crystal was first evident in 1997, when observed by Fichou and co-workers[8] for an octylthiophene crystal. Later, other ASE experiments have been reported on conjugated oligomeric crystalline materials including an oligo(*p*-phenylenevinylene),[9] oligothiophene,[10]

[*] Dr. N. Mercier, Dr. X. Zhu, Prof. P. Frère
Laboratoire IMMO, UMR-CNRS 6501
Université d'Angers
2 Bd Lavoisier, F-49045 Angers (France)
E-mail: nicolas.mercier@univ-angers.fr
Prof. J. M. Nunzi, Dr. D. Gindre
Laboratoire POMA, UMR-CNRS 6136
Université d'Angers
2 Bd Lavoisier, F-49045 Angers (France)
E-mail: jean-michel.nunzi@univ-angers.fr
Dr. X. Zhu
Institute of Advanced Materials and Technology
Fudan University
220 Handan Rd, Shanghai 200433 (P.R. China)

[**] We thank the Pays de la Loire region for a post-doc fellowship to X. H. Z.

  DOI: 10.1002/adma.200304816